



High-Speed Railway Fastener Detection Based on a Line Local Binary Pattern

Hong Fan , Pamela C. Cosman , *Fellow, IEEE*, Yun Hou, and Bailin Li

Abstract—Traditional image features are not able to effectively represent railway fasteners under varied illumination and conditions. We propose the line local binary pattern encoding method that considers the relationship between the center point and its upper and lower neighborhoods. The method can effectively represent the key components of fasteners. In comparison with several state-of-the-art methods, the proposed method has good performance on detecting the completely missing and partly missing fasteners on real data sets, especially when the illumination and background are not ideal.

Index Terms—Image classification, local binary pattern (LBP), railway fasteners, railway maintenance, visual inspection.

I. INTRODUCTION

RAILWAY fastener failures affect train smoothness, increase wear on rails and wheels, and affect safety. Fastener detection is an important task for railway maintenance. However, traditional manual detection is slow, costly, and even dangerous. In recent years, with the development of high-speed railways, the automatic fastener detection technology based on machine vision is receiving more attention [1]–[10].

Singh *et al.* [1] use edge density to locate the clips and detect the missing clips, then detect the recently replaced blue clips based on color information in the located window. De Ruvo *et al.* [2]–[7] begin by finding the fastener window according to the prior geometric relationship of the railway components. De Ruvo *et al.* [2] and Marino *et al.* [4] then detect missing fasteners with a multilayer perceptron neural network classifier based on wavelets. Mazzeo *et al.* [3] and Stella *et al.* [5] detect the missing fasteners with a back-propagation (BP) neural network and an radial basis function (RBF) neural network classifier based on wavelets and principal component analysis. Xia *et al.* [6] divide the fastener into four parts, and train each part independently

Manuscript received December 1, 2017; revised March 31, 2018; accepted April 2, 2018. Date of publication April 12, 2018; date of current version April 26, 2018. This work was supported in part by the National Science Foundation of China under Grant 51275431; and in part by the Sichuan Province Science and Technology Support Program Project under Grant 2016GZ0194. The associate editor coordinating the review of this manuscript and approving it for publication was Dr. Sumohana S. Channappayya. (*Corresponding author: Hong Fan.*)

H. Fan, Y. Hou, and B. Li are with the School of Mechanical Engineering, Southwest Jiaotong University, Chengdu 610031, China (e-mail: hg.fan@foxmail.com; 672384055@qq.com; blli62@263.net).

P. C. Cosman is with the Department of Electrical and Computer Engineering, University of California, San Diego, CA 92093-0407 USA (e-mail: pcosman@eng.ucsd.edu).

Color versions of one or more of the figures in this letter are available online at <http://ieeexplore.ieee.org>.

Digital Object Identifier 10.1109/LSP.2018.2825947

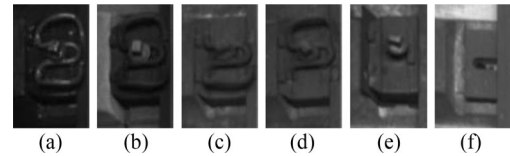


Fig. 1. Examples of fasteners. (a)–(b) Normal fastener. (c)–(d) Partly missing fasteners. (e)–(f) Completely missing fasteners.

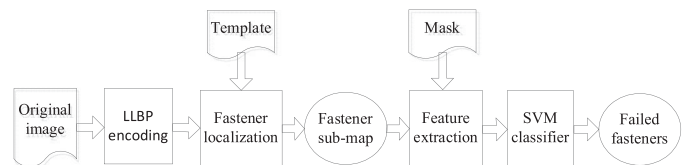


Fig. 2. Flow diagram of the proposed method.

by AdaBoost based on Haar-like features. Liu *et al.* [7] use a sparse representation algorithm to recognize two symmetrical fasteners using the pyramid histogram of oriented gradients. Similarly, Yang *et al.* [8] extract the direction field as the feature descriptor of fasteners, and detect missing fasteners by weighted template matching. Li *et al.* [9] locate the fastener region by the Hough transform, and then detect missing fasteners based on edge features. Feng *et al.* [10] locate the fastener area based on the geometric relationship between the tie (sleeper), rail and fastener, and then detect partially worn and completely missing fasteners using a probabilistic topic model based on Haar-like features.

However, most of these algorithms can only detect the completely missing fasteners, not partly missing fasteners, and the robustness to illumination variation and weather change was not discussed. Also, the fastener area is located with low accuracy, due to the lack of effective description operators. Underlying features including histogram of oriented gradient (HOG), local binary pattern (LBP), edge, and Haar-like features are usually used in these algorithms. However, these features do not account for particularities of the fasteners, so they are not able to effectively represent its key parts, especially when the illumination, weather, and other external environment change.

In this letter, an algorithm for high-speed railway fastener detection is proposed based on the line local binary pattern (LLBP), which can effectively distinguish between normal fasteners and failed fasteners (completely missing and partly missing, as shown in Fig. 1). The proposed method is robust to illumination, weather, railway conditions, and complex background. The flow diagram of the method is shown in Fig. 2. Due

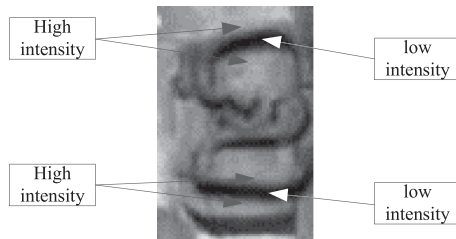
Fig. 3. Neighborhood structure of the LBP (for $n = 8$).

Fig. 4. Grayscale characteristics of the fastener image.

to space limitations, this letter considers only one very common type of fastener used in high-speed railways. However, our method also performs well on fasteners with other shapes.

II. PROPOSED METHOD

In this section, we first provide a brief review of the local binary pattern. We then propose the LLBP algorithm and a method of extracting features for fastener detection.

A. Brief Review of the LBP

The original LBP operator, proposed by Ojala *et al.* [11], compares the central pixel and the surrounding neighborhood. Given a central pixel g_c and its neighborhood of n pixels, if the neighborhood point $g_n > g_c$, then its bit is recorded as 1, otherwise 0. The LBP value of the central point is the weighted sum of each bit. Formally, the basic LBP operator at a given center pixel is defined as

$$\text{LBP}_{N,R} = \sum_{n=0}^{N-1} s(g_n - g_c) 2^n \quad (1)$$

where

$$s(x) = \begin{cases} 1, & \text{if } x \geq 0 \\ 0, & \text{if } x < 0 \end{cases} \quad (2)$$

where g_c and g_n are, respectively, the gray values of the central pixel p_c and its neighbors p_n ($n = 0, 1, \dots, N - 1$), as illustrated in Fig. 3.

B. Proposed LLBP

The incident angle of the illumination is fixed (because high-speed railways are typically inspected at night) and the fastener structure too, so there is an inherent grayscale relationship in the key area of the fastener, as shown in Fig. 4.

The original LBP is not able to effectively represent the grayscale characteristic of the fastener because it considers the

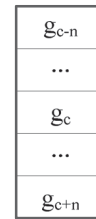


Fig. 5. Neighborhood structure of the LLBP.

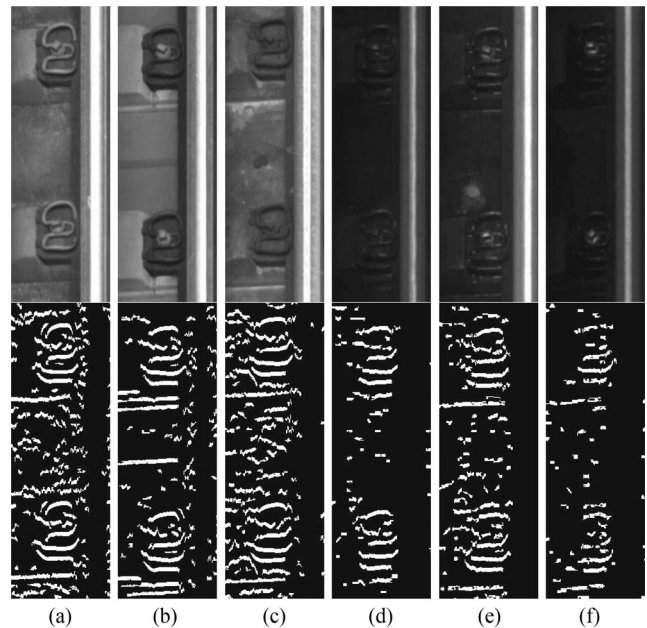


Fig. 6. Fastener images and their corresponding LLBP coded maps in different conditions. (a) White fastener. (b) New railway. (c) Old railway. (d) Low illumination. (e) Rainy. (f) Low illumination + rainy.

relationship between the center point and the entire neighborhood, while only points above and below contribute useful information, and the left and right points do not. Based on this, we propose a new local neighborhood encoding method, called the line LBP, which considers the relationship between the center point and its upper and lower neighbors as

$$\text{LLBP}_n = s(g_{c-n} - g_c) \times s(g_{c+n} - g_c) 2^0 \quad (3)$$

where g_c and $g_{c\pm n}$ are the gray values of the central pixel p_c and its neighbors $p_{c\pm n}$, respectively, as illustrated in Fig. 5.

The LLBP has one parameter n , which determines the size of the neighborhood. As n becomes larger, the contour of the fastener gets thicker. Small values of n will cause feature extraction to be unstable. If the value of n is too large, it will reduce the accuracy of fastener positioning, while introducing noise in the nonfastener area. Original fastener images and their corresponding LLBP coded maps in different conditions with $n = 6$ are shown in Fig. 6. The Fastener images encoded by the LLBP with different values of n are shown in Fig. 7.

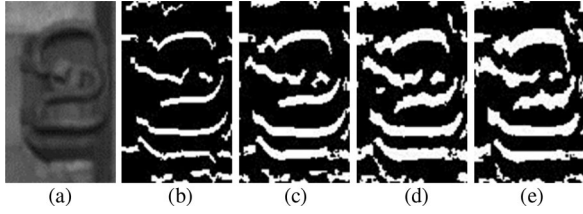


Fig. 7. Fastener images coded by the improved LBP with different values of n . (a) Original image. (b) $n = 4$. (c) $n = 6$. (d) $n = 8$. (e) $n = 10$.

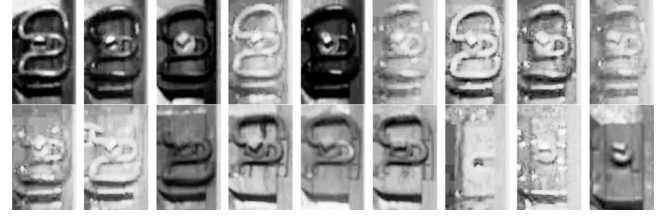


Fig. 10. Submap for the fastener recognition.



Fig. 8. Images for the fastener localization.

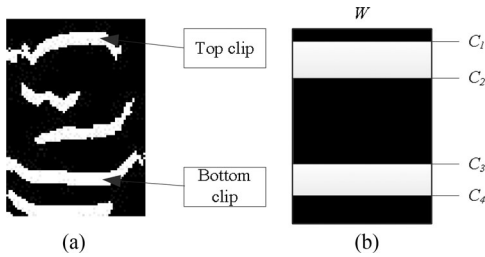


Fig. 9. Fastener template and its corresponding mask. (a) Template. (b) Mask.

C. Fastener Feature Extraction

1) *Fastener Localization*: The precise region of the fastener is obtained by the template matching algorithm, which uses the sum of absolute differences (SAD) as the metric [12]. The SAD template matching formula is as follows:

$$D(i, j) = \frac{1}{M \times N} \sum_{s=1}^M \sum_{t=1}^N |S(i+s-1, j+t-1)T(s, t)| \quad (4)$$

where $1 \leq i \leq m - M + 1, 1 \leq j \leq n - N + 1$ and $S(x, y)$ is the searching image with the size of $m \times n$, which is obtained by encoding the original image (see Fig. 8) with the LLBP. $T(x, y)$ is the fastener template of size $M \times N$. The template used in this letter is shown in Fig. 9(a), which is a region of a normal fastener image encoded by the LLBP. D is a similarity matrix of size $(m - M + 1) \times (n - N + 1)$. To get the position of the fastener in the original image, we only need to find the position of the smallest element in matrix D . Based on the fastener location and the template's size, we can easily capture

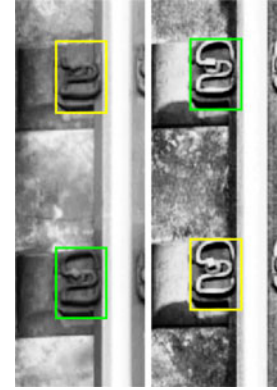


Fig. 11. Examples of a fastener matching result.

the fastener submap (see Fig. 10) from the original image. The result of fastener matching is shown in Fig. 11.

2) *Fastener Feature Description*: In order to calculate the features of key fastener parts, we generate a mask K based on the fastener template, which has the same size as the template. It is necessary to ensure that the white area of the mask can cover the key areas of the fastener, which include the top and bottom clips, as shown in Fig. 9(b).

We use the areas of the top and bottom clips to represent their features, which are covered by the template and mask. The formula is

$$f_1 = \sum_{i=c_1}^{c_2} \sum_{j=1}^W (I(i, j) \cdot T(i, j)) / N_1 \quad (5)$$

$$f_2 = \sum_{i=c_3}^{c_4} \sum_{j=1}^W (I(i, j) \cdot T(i, j)) / N_2 \quad (6)$$

where

$$N_1 = \sum_{i=c_1}^{c_2} \sum_{j=1}^W (K(i, j) \cdot T(i, j)) \quad (7)$$

$$N_2 = \sum_{i=c_3}^{c_4} \sum_{j=1}^W (K(i, j) \cdot T(i, j)) \quad (8)$$

where I is the fastener submap encoded by the LLBP, W is the mask width, and c_i is the mask vertical coordinates as shown in Fig. 9(b). Given mask and template, N_1 and N_2 , are constant. The values of f_1 and f_2 are between 0 and 1 with higher values meaning it is more likely the clip is present. We determine whether the upper and lower clips are missing by f_1 and f_2 . If

TABLE I
LR ON RAIL FASTENER

APPROACH	Localization rate(LR)
Yang's[6]	92.45%
Xia's[7]	88.74%
Feng's[10]	95.36%
Ours($n=4$)	99.62%
Ours($n=6$)	99.98%
Ours($n=8$)	99.24%
Ours($n=10$)	98.15%

the top and bottom clips are missing at the same time, it means that the entire fastener is missing.

Algorithm for Fastener Feature Extraction

- Step 1: Give the value of n and template T and mask K ;
 Step 2: Encode the original image by the LLBP according to (3);
 Step 3: Match the LLBP image with fastener template to locate the fastener region according to (4);
 Step 4: Compute the features of top clip and bottom clip, respectively, according to (5) and (6);

III. EXPERIMENTAL RESULTS

The experiments are organized in two sections. First, we compare the LLBP operator with other methods proposed for the fastener localization. Next, using the fastener submap obtained by our localization method, we compare the recognition results obtained by the proposed features to the ones obtained by the LBP histogram and LBP variants, including LBP [11], local ternary pattern (LTP) [13], completed local binary pattern (CLBP) [14], center-symmetric local binary pattern (CSLBP) [15], and noise-resistant local binary pattern (NRLBP) [16].

We carried out the two experiments on our own public railway image database (<https://pan.baidu.com/s/1hs1q15U>) obtained by a line scan camera on a high-speed railway in real-world environments. The database has 6000 images, including 4000 normal fasteners, 1000 partly missing fasteners, and 1000 completely missing fasteners. The railway images in the database are obtained in various environments, including new and old railways, rainy days, and various illumination conditions.

In the first experiment, the database images (size 820×350) were used directly as an input (see Fig. 8). The template image (size 104×64) is shown in Fig. 9(b). If the location obtained by the fastener localization is less than four pixels from the true position (as determined manually) in both horizontal and vertical directions, then it is defined as correct location. The localization rate (LR), reported in Table I, is the percentage of fasteners that are correctly located. We evaluated the performance of our fastener localization method with different values of n and compared to three state-of-the-art methods.

From Table I, we observe that our fastener localization method (for $n = 6$) achieves higher correct localization than other methods. When n is approximately equal to the height of

TABLE II
RECOGNITION RATE ON A FAILED RAIL FASTENER

APPROACH	Recall	Precision
LBP	95.86%	96.42%
LTP	99.17%	98.75%
CLBP	99.25%	98.90%
CSLBP	96.24%	97.97%
NRLBP	96.75%	93.38%
LLBP	100%	99.8%

the low intensity region, the LLBP accurately represents the low intensity region and introduces less extraneous information.

In the second experiment, we evaluated the performance of different features with a linear support vector machine (SVM) classifier based on the fastener submap obtained by our localization method. The size of the submap is 104×64 , as shown in Fig. 10, and the other parameters are set as $n = 6$, $c_1 = 21$, $c_2 = 31$, $c_3 = 73$, and $c_4 = 83$. We use the standard definitions of Recall = tp/N and Precision = $tp/(tp + fp)$ to evaluate the performance of different features where tp is the number of correctly classified samples for a class, fp is the number of false positives (incorrectly classified samples), and N is the total number of test samples for this class.

In the dataset, the completely missing fasteners and the partly missing fasteners are labeled as one class. The dataset is divided in ten groups and we use nine groups as training set and the one group left out is used as the test set. This was repeated ten times, with a different group left out each time, and the results are averaged and reported in Table II. All the features achieve good precision–recall performance but our proposed feature achieves a better performance than the others. The reason is that our fastener localization method provides an accurate fastener submap for the subsequent classification and our feature effectively represents the grayscale characteristic of the fastener. Although our recall and precision only increased slightly in numerical values, the improvement in engineering applications is worthwhile due to the large numbers of fasteners. For example, there are almost 7000 fasteners per kilometer of railway.

Another advantage of our features is that the computational complexity is lower than for other features, as ours are based on the image coded by the LLBP, already calculated in the previous fastener localization process.

IV. CONCLUSION

The detection of failed fasteners is an important task in railway maintenance. In this letter, a new algorithm for detecting the high-speed railway fasteners was proposed. Relying on the LLBP feature, the proposed algorithm can simply and reliably detect the failed fasteners in different environments. As fastener localization is effective, the subsequent processing steps are greatly simplified. The experimental results show that the proposed method has very high performance on detecting the fully and partly missing fasteners. The features presented in this letter are very effective for fastener images, and can also be used for other targets with similar illumination characteristics.

REFERENCES

- [1] M. Singh, S. Singh, J. Jaiswal, and J. Hemphshall, "Autonomous rail track inspection using vision based system," in *Proc. Int. Conf. IEEE Comput. Intell. Homeland Security Personal Safety*, Oct. 2006, pp. 56–59.
- [2] P. de Ruvo, A. Distante, E. Stella, and F. Marino, "A GPU-based vision system for real time detection of fastening elements in railway inspection," in *Proc. 16th Int. Conf. IEEE Image Process.*, Nov. 2009, pp. 2333–2336.
- [3] P. L. Mazzeo, M. Nitti, E. Stella, and A. Distante, "Visual recognition of fastening bolts for railroad maintenance," *Pattern Recognit. Lett.*, vol. 25, no. 6, pp. 669–677, Apr. 2004.
- [4] F. Marino, A. Distante, P. L. Mazzeo, and E. Stella, "A real-time visual inspection system for railway maintenance: Automatic hexagonal-headed bolts detection," *IEEE Trans. Syst., Man, Cybern. C, Appl. Rev.*, vol. 37, no. 3, pp. 418–428, May 2007.
- [5] E. Stella, P. Mazzeo, M. Nitti, G. Cicirelli, A. Distante, and T. D'Orazio, "Visual recognition of missing fastening elements for railroad maintenance," in *Proc. Int. Conf. IEEE Intell. Transp. Syst.*, Sep. 2002, pp. 94–99.
- [6] Y. Xia, F. Xie, and Z. Jiang, "Broken railway fastener detection based on adaboost algorithm," in *Proc. Int. Conf. Optoelectron. Image Process.*, Nov. 2010, vol. 1, pp. 313–316.
- [7] J. Liu, B. Li, J. Luo, and L. Li, "Integrating the symmetry image and improved sparse representation for railway fastener classification and defect recognition," *Math. Problems Eng.*, vol. 2015, Oct. 2015, Art. no. 462528.
- [8] J. Yang, W. Tao, M. Liu, Y. Zhang, H. Zhang, and H. Zhao, "An efficient direction field-based method for the detection of fasteners on high-speed railways," *Sensors*, vol. 11, no. 8, pp. 7364–7381, Jul. 2011.
- [9] Y. Li, C. Otto, N. Haas, Y. Fujiki, and S. Pankanti, "Component-based track inspection using machine-vision technology," in *Proc. 1st Int. Conf. ACM Multimedia Retrieval*, 2011, Art. no. 60.
- [10] H. Feng, Z. Jiang, F. Xie, P. Yang, and J. Shi, "Automatic fastener classification and defect detection in vision-based railway inspection systems," *IEEE Trans. Instrum. Meas.*, vol. 63, no. 4, pp. 877–888, Apr. 2014.
- [11] T. Ojala, M. Pietikainen, and T. Maenpaa, "Multiresolution gray-scale and rotation invariant texture classification with local binary patterns," *IEEE Trans. Pattern Anal. Mach. Intell.*, vol. 24, no. 7, pp. 971–987, Jul. 2002.
- [12] A. R. Rao and B. G. Schunck, "Computing oriented texture fields," in *Proc. IEEE Comput. Soc. Conf. Comput. Vision Pattern Recognit.*, Jun. 1989, pp. 61–68.
- [13] X. Tan and B. Triggs, "Enhanced local texture feature sets for face recognition under difficult lighting conditions," *IEEE Trans. Image Process.*, vol. 19, no. 6, pp. 1635–1650, Jun. 2010.
- [14] Z. Guo, L. Zhang, and D. Zhang, "A completed modeling of local binary pattern operator for texture classification," *IEEE Trans. Image Process.*, vol. 19, no. 6, pp. 1657–1663, Jun. 2010.
- [15] R. Gupta, H. Patil, and A. Mittal, "Robust order-based methods for feature description," in *Proc. Int. Conf. IEEE Comput. Vision Pattern Recognit.*, 2010, pp. 334–341.
- [16] J. Ren, X. D. Jiang, and J. Yuan, "Noise-resistant local binary pattern with an embedded error-correction mechanism," *IEEE Trans. Image Process.*, vol. 22, no. 10, pp. 4049–4060, Jun. 2013.